ACCSCIENCE PUBLISHING

Global Translational Medicine

ORIGINAL RESEARCH ARTICLE

Models for non-invasive fetal electroencephalogram signal extraction during gestation

Eden Koresh[1†], Ophir Oren[1†], Offer Erez[2,3,4*], Ali Nasirlou[2†], Eilon Shany[5], Robert Clancy[6], Yaniv Zigel[1], Taeer Avnon[7], and Allon Guez[8]

[1]Department of Biomedical Engineering, Faculty of Engineering, Ben Gurion University of the Negev, Beer Sheva, Israel

[2]FetalEEG Inc., Penn Valley, Pennsylvania, United States of America

[3]Department of Obstetrics and Gynecology, Soroka University Medical Center, Ben Gurion University of the Negev, Beer Sheva, Israel

[4]Department of Obstetrics and Gynecology, School of Medicine, Wayne State University, Detroit, Michigan, United States of America

[5]Department of Neonatology, Soroka University Medical Center, Ben Gurion University of the Negev, Beer Sheva, Israel

[6]Department of Pediatrics, The Children's Hospital of Philadelphia, University of Pennsylvania School of Medicine, Philadelphia, Pennsylvania, United States of America

[7]School of Medicine, Ben Gurion University of the Negev, Beer Sheva, Israel

[8]Department of Electrical Engineering, College of Engineering, Drexel University, Philadelphia, Pennsylvania, United States of America

[†]*These authors contributed equally to this work.*

***Corresponding author:**
Offer Erez
(erezof@bgu.ac.il)

Citation: Koresh E, Oren O, Erez O, *et al*. Models for non-invasive fetal electroencephalogram signal extraction during gestation. *Global Transl Med*. 2025;4(4):90-105. doi: 10.36922/GTM025260052

Received: June 24, 2025

1st revised: October 17, 2025

2nd revised: October 31, 2025

Accepted: November 4, 2025

Published online: December 22, 2025

Abstract

The functional development of the fetal brain is critical for long-term health, yet current diagnostic tools lack the capability to examine it effectively. This paper presents a non-invasive method for extracting fetal brain signals using abdominal recordings obtained before elective cesarean sections, with neonatal brain activity recorded post-delivery serving as a reference. The recorded abdominal signals were preprocessed using digital filters and separated into independent components using the blind source separation technique: Independent component analysis. These components were analyzed to identify potential fetal brain signals based on their similarity to postnatal brain activity and dissimilarity to maternal cardiac signals, which are the primary source of interference in abdominal recordings. Features related to time and frequency characteristics were extracted, and a feature selection was conducted to identify the most informative ones. Preliminary results using simulated data demonstrated effective signal separation, with some segments closely resembling postnatal brain activity in spectral features. Low-frequency bands showed the strongest potential for distinguishing fetal brain activity from maternal interference. This approach demonstrates a feasible pathway for non-invasive fetal brain monitoring with implications for early detection of neurological development issues.

Keywords: Fetal brain function; Neonatal electroencephalogram; Signal processing; Non-invasive monitoring; Independent component analysis; Frequency-domain analysis; Cesarean section

1. Introduction

The developmental trajectory of the fetal brain is crucial to an individual's lifelong health and cognitive capabilities. From conception through early adulthood, the brain evolves and undergoes critical growth phases, establishing the neural foundations for future cognitive, mental, and physical functions.[1] However, the ability to monitor and assess these functional developmental processes *in utero* poses significant challenges due to the limitations of current diagnostic technologies. Conventional prenatal imaging methods, such as fetal ultrasound and magnetic resonance imaging, are designed to examine anatomical rather than functional features.[2] This limitation often results in failures to detect subtle yet crucial functional aspects of the fetal brain with normal anatomical structure.[3] Consequently, many neurodevelopmental conditions that are diagnosed among children who had a normal pregnancy and those who develop cerebral palsy and developmental delays related to preterm birth or fetal growth restrictions are not identified early enough to initiate timely intervention.[4,5] Traditional monitoring systems such as fetal heart rate tracing, despite being widely used during labor to evaluate fetal wellbeing, have not significantly reduced the incidence of fetal brain injuries.[6] The lack of effective, non-invasive tools for functional monitoring of the fetal brain represents a significant gap in prenatal care. This highlights an urgent unmet need for innovative solutions that can provide deeper insights into functional fetal neurodevelopment without compromising the safety of the developing fetus.[6] However, non-invasive monitoring techniques (e.g., fetal electroencephalogram [fEEG] tracing) face technological challenges, such as low signal-to-noise ratio (SNR). This leads to challenges with artifact filtration, due to the low amplitude of fetal brain signals and significant noise interference (e.g., maternal and environmental noise).

Historically, the exploration of fetal brain activity has been pursued through invasive methods and non-invasive techniques such as fetal magnetoencephalography and fEEG. The initial non-invasive fEEG report was a case study by Lindsley,[7] who examined his unborn child in the third trimester using abdominal probes, but the data were severely compromised by artifacts. Subsequent enhancements by Bernstine *et al.*[8] in 1955, and later Rosen *et al.*[9] in 1973, introduced the use of scalp electrodes which improved signal clarity but still faced issues, such as interference from maternal and fetal movement. Despite improvements, these methods did not adequately address the low SNR and the challenge of distinguishing fetal brain activity from other physiological sources. Eswaran *et al.*[10] made notable advances using a combination of fetal heart rate scalp electrodes and standard monitoring equipment to detect auditory evoked potentials, yet the approach still struggled with ambient noise and signal attenuation. This historical progression illustrates a pattern of incremental advancements yet persistent technological shortcomings that prevent effective electrophysiological monitoring. To address these gaps, we aim to conduct a proof-of-concept study to develop a non-invasive method to extract fEEG during gestation prior to the onset of labor as an indicator of fetal brain function and activity. The method will be evaluated for its ability to reliably isolate fEEG signals from non-invasive abdominal recordings, characterize their spectral and temporal features, and assess their potential for detecting patterns associated with fetal neurological activity.

2. Materials and methods

2.1. Materials

Three types of electroencephalogram (EEG) acquisition machines were assessed in this study:

(i) Brain Vision: Included eight leads EEG (FP_1, FP_2, C_3, C_4, T_3, T_4, O_1, O_2 according to the 10–20 system), two respiratory channels, and two electrocardiogram (ECG) channels sampled at 250 Hz with 16-bit resolution.

(ii) Bio-Logic Netlink EEG: Included eight leads EEG (for neonatal recordings, electrodes were positioned at FP_1, FP_2, C_3, C_4, T_3, T_4, O_1, O_2 according to the 10–20 system), one respiratory channel, and one ECG channel sampled at 256 Hz with 16-bit resolution.

(iii) X-trodes XTR EEG16: Included 16 EEG leads (AF_7, AF_8, FP_1, FP_2, L_1, L_3, L_4, L_5, L_8, R_1, R_3, R_4, R_5, R_8, E_1, E_2) sampled at 250 Hz with 16-bit resolution.

We tested three EEG acquisition systems to balance clinical relevance, neonatal feasibility, and advanced signal quality, and to identify the most suitable platform for this innovative research. The Brain Vision system (Brain Products GmbH, Germany) enabled reliable multimodal recordings (EEG, respiration, ECG) in a controlled setting. The BioLogic Netlink EEG (Natus Medical Inc., USA) reflected standard neonatal clinical practice, ensuring translational relevance. The Xtrodes XTR EEG16 (Xtrodes Ltd., Israel) provided a novel wearable solution with a higher channel count for improved spatial resolution and flexible placement. This multi-system approach ensured robust validation and guided selection of the optimal system for our study.

For the recordings conducted before delivery, we selected the BioLogic Netlink EEG and used it consistently for both the maternal and neonatal recordings. This approach ensured methodological consistency and minimized potential bias arising from differences in device performance.

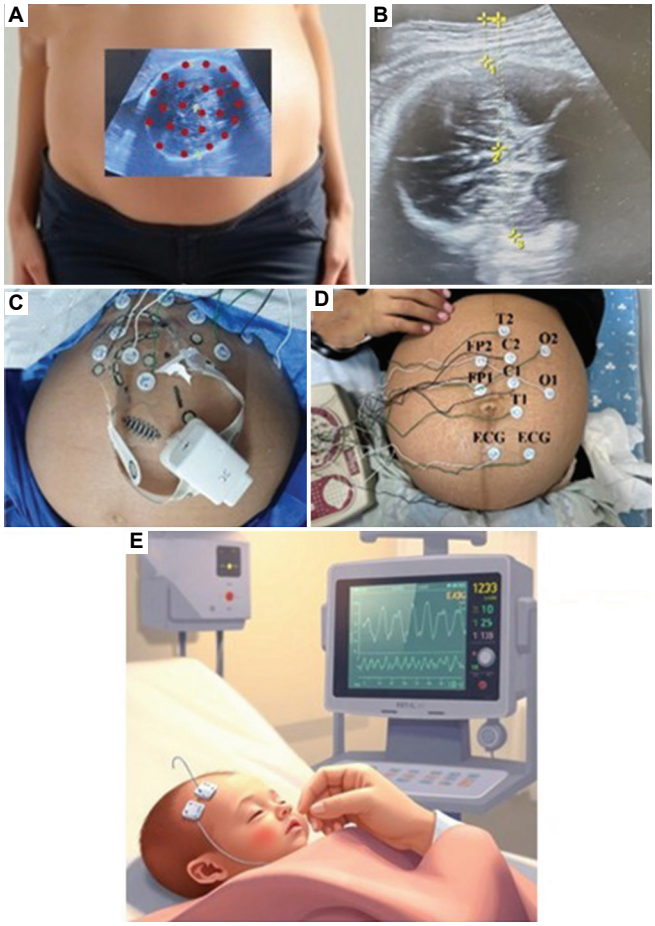

Figure 1. Illustration of the approach used to acquire the neonatal electroencephalogram and the transabdominal multi-channel electroencephalogram (mcECG). (A) Ultrasound imaging is used to determine fetal head positioning and to specify electrode arrangement. (B) Measurement of fetal brain distance from the maternal abdominal wall. (C and D) Electrode array placement on the mother's abdomen for mcEEG recording. (E) Neonatal electroencephalogram acquisition. Images A and E are artificial intelligence-generated; the ultrasound and the placement of maternal abdominal electrodes are from patients enrolled in the study.

2.2. Data acquisition

This study was an observational cohort study. The study cohort was recruited among women scheduled for elective cesarean section who signed an informed consent form at the Soroka University Medical Center. We collected the data from women before elective cesarean section without labor, and all women had the cesarean section at term, between 38 and 40 weeks of gestation. The women recruited to the study had low-risk pregnancies without any complications or maternal diseases. They had regional anesthesia during an elective section without contractions or signs of labor. Inclusion criteria: Normal pregnancy, scheduled cesarean delivery without labor, and spinal anesthesia during surgery. Exclusion criteria: women with pregnancy complications, any signs of labor process (uterine contractions, rupture of membranes, effacement and dilatation of the cervix), general anesthesia during surgery, fetal anomalies, or chromosomal abnormalities. The study was approved by the local institutional review board at the Soroka University Medical Center. In the current study, we included 20–40 min of EEG recordings from two mothers and two 20–40 min of neonatal EEG (nEEG) recordings from their neonates after delivery. To improve signal quality, we first localized the fetal head using ultrasound and placed the electrodes accordingly (Figures 1A and B), maximizing the likelihood of capturing fetal brain activity while minimizing noise. The first recording included an array of electrodes placed on the maternal abdomen before delivery to record multi-channel EEG (mcEEG) signals. We performed an ultrasound examination to identify the position of the fetus and the exact location of the fetal skull/brain. We then marked on the maternal abdomen the location of the fetal skull and placed the EEG electrodes accordingly (Figures 1C and D). The second recording is

of the neonate; it was performed within 24 h post-partum and provided a direct measure of the nEEG signals (Figure 1E). These nEEG signals served as a reference, assuming their patterns and frequencies resemble those of fEEG.[11] Up to 15 mcEEG and nEEG signals were recorded by clinicians at the Maternity Center, Soroka Medical Center.

2.3. Signal preprocessing and source separation

After acquiring the mcEEG and nEEG signals, preprocessing was applied using digital filters: A fourth-order Butterworth high-pass filter with a cutoff frequency of 0.5 Hz and a second-order Butterworth low-pass filter with a cutoff frequency of 70 Hz to minimize residual artifacts. These frequencies comply with the nEEG recordings recommendations of the American Clinical Neurophysiology Society.[12] Furthermore, a 50 Hz infinite-impulse-response notch filter was applied to eliminate powerline hum. Those filters were designed using MATLAB (R2024a, MathWorks, Inc., USA). The fast independent component analysis (ICA) algorithm operates iteratively to minimize mutual information while maximizing non-Gaussianity for source separation.[13] The key assumption behind ICA is that the observed data is a linear mixture of the primary sources (Equation 1):

$$\mathbf{X} = \mathbf{AS} \tag{1}$$

where $\mathbf{X}$ is the observed mixed signal matrix after filtering and centering, $\mathbf{A}$ is the mixing matrix (which is unknown), and $\boldsymbol{S}$ is the matrix of independent source signals. The objective is to estimate the unmixing matrix $\mathbf{W}$ to be as close as possible to the inverse of $\mathbf{A}$, by maximizing a measure of non-Gaussianity, such as negentropy (Equation 2):

$$J(y) = H(y_G) - H(y) \tag{2}$$

Where $H(y_G)$ represents the entropy of a Gaussian distribution (y_G), and $H(y)$ is the entropy of the observed signal. The iterative update of the unmixing matrix was accomplished using the gradient ascent rule (Equation 3):

$$\mathbf{w}_{\text{new}} = \mathbb{E}\left[\mathbf{x}J\left(\mathbf{w}^{\mathrm{T}}\mathbf{x}\right)\right] - \mathbb{E}\left[J'\left(\mathbf{w}^{\mathrm{T}}\mathbf{x}\right)\right]\mathbf{w} \tag{3}$$

where $\mathbb{E}[.]$ denotes the expectation operator and $J'(\cdot)$ is the first derivative of $J(\cdot)$–the negentropy. This facilitates the convergence towards weight vectors w that effectively separate independent components. The end goal is that the linear transformed data is an evaluation of the hidden sources (Equation 4):

$$\tilde{\mathbf{S}} = \mathbf{WX} \tag{4}$$

so $\tilde{\mathbf{S}}$ will be as close as possible to the real sources.

To validate the robustness of the FastICA algorithm, preliminary simulations were conducted before its application to our dataset. Signals from mcEEG were emulated by utilizing four primary sources: Single-channel nEEG and ECG recorded using the Brain Vision device, and adult ECG and electromyogram (EMG) obtained from "Physionet."[14,15] The neonatal signals represent the fetal signals, while those from the adults represent the physiological maternal noises. Signal amplitudes were adjusted to approximate those observed in experimental data and literature sources.[16,17] This deliberate exaggeration aimed to stress-test the FastICA algorithm under non-standard conditions. Multiple simulations were conducted with random mixing to generate varied mcEEG signals while preserving approximated signal ratios. To obtain quantitative results, the normalized mean square error (NMSE) was employed (Equation 5).

$$NMSE = \frac{\sum_{i=1}^{N}\left(\hat{\mathbf{x}}_i - \mathbf{x}_i\right)^2}{\sum_{i=1}^{N}\left(\mathbf{x}_i - \bar{\mathbf{x}}\right)^2} \tag{5}$$

where $\hat{\mathbf{x}}$ is the ICA output signal (component), $\mathbf{x}$ represents the original signal, $\bar{\mathbf{x}}$ denotes the mean of the original signal, and N is the number of samples. A lower NMSE value indicates a higher similarity between the signals.

2.4. Feature extraction

Following ICA on the mcEEG signals, each ICA component and nEEG signal were segmented into 20-s intervals for frequency- and time-domain feature extraction.

Five frequency-domain features were considered, while only 2 time-domain features were used. Although several time-domain features are commonly used in nEEG analysis, such as average, standard deviation, magnitude, synchrony, and discontinuity,[18] they were excluded due to the limitations of ICA, which does not preserve magnitude and introduces a permutation problem.[13] In addition, although the amplitude range for intrapartum fEEG recordings has been reported to range from 5 to 50 μV,[19] the amplitude of antepartum fEEG remains unknown due to signal attenuation caused by the distance between the fetal brain and the maternal abdominal wall. Therefore, these time-domain features could not be reliably applied in our analysis.

2.4.1. Relative spectral power (RSP)

Multiple studies have shown that fEEG wave frequencies range from 0.5 to 25 Hz.[19,20] However, based on evidence that fEEG patterns resemble postnatal nEEG,[3] we adopted the standard nEEG wavebands for our analysis. These bands were: 0.5–3 Hz (δ), 3–8 Hz (θ), 8–15 Hz

(α), 15–30 Hz (β), and 30–48 Hz (γ).[21] Using these bands allowed us to extract frequency domain features consistently with nEEG studies, including the RSP feature, which is the ratio between the sum of the power within a specific frequency band and the total power across all frequencies in each signal (Equation 6):

$$RSP = \frac{\sum_{k \in range} \mathbf{PSD}_k}{\sum_k \mathbf{PSD}_k} \tag{6}$$

Power was estimated by the power spectral density (PSD) using the "periodogram" function in MATLAB.

2.4.2. Autoregressive (AR) coefficients

In an AR model, a time series corrupted by white noise is predicted based on its own past values. Mathematically, it can be represented as a linear filter (Equation 7).[22]

$$\mathbf{x}(n) = -\sum_{i=1}^{p} a_p(i)\mathbf{x}(n-i) + \boldsymbol{\varepsilon}(n) \tag{7}$$

where **x** is a signal, p is the AR order, **ε** is the white noise and $a_p(i)$ is the AR coefficients that were incorporated into the feature vector. The "arburg" function in MATLAB was used to estimate the AR coefficients. The order of the model p was chosen to be 10.

2.4.3. Intensity weighted mean frequency

This feature provides the average frequency from the PSD, offering a sense of overall frequency distribution. It reflects where the majority of the power is concentrated (Equation 8):[23]

$$IWMF = \frac{\sum_k \mathbf{PSD}_k \mathbf{f}_k}{\sum_k \mathbf{PSD}_k} \tag{8}$$

where **f** is the frequency vector.

2.4.4. Intensity weighted bandwidth

This feature indicates the dispersion of power around the mean frequency (Equation 9):[23]

$$IWBW = \sqrt{\sum_k \mathbf{PSD}_k \left(\mathbf{f}_k - IWMF\right)^2} \tag{9}$$

2.4.5. Spectral edge frequency (SEF)

The frequency at which a certain percentage (α) of the total power in the normalized PSD is reached is defined as $\mathbf{f}_{SEF}$ (Equation 10).[23] For instance, the SEF 50 is equivalent to the median frequency.[24] In this study, we chose $\alpha = 90$.

$$\sum_{\mathbf{f}_k=0}^{\mathbf{f}_{SEF}} \mathbf{PSD}_k = \frac{\alpha}{100} \tag{10}$$

2.4.6. Mean absolute of the first differences

This measure captures the average magnitude of change between consecutive samples. The mean absolute of the first differences is a simple yet effective statistic for assessing local fluctuations in time-series data, and we used it to quantify short-term variability in the signal (Equation 11).

$$MAFD = \frac{1}{N-1}\sum_{i=1}^{N-1}\left|\mathbf{x}_{i+1} - \mathbf{x}_i\right| \tag{11}$$

2.4.7. Mean absolute of the second differences

This feature measures the average magnitude of the signal's acceleration, which represents how quickly the first differences change between consecutive samples. This statistic is useful for characterizing local smoothness and short-term curvature in time-series data. We used it to evaluate variability in the signal's rate of change (Equation 12).

$$MASD = \frac{1}{N-2}\sum_{i=1}^{N-2}\left|\mathbf{x}_{i+2} - 2\mathbf{x}_{i+1} + \mathbf{x}_i\right| \tag{12}$$

where **x** is the signal and N denotes the number of samples in Equations 11 and 12.

2.5. Feature selection and statistical analysis

The feature selection process was conducted in two stages to identify the most effective features for distinguishing fEEG from noisy signals. Given the established pattern similarities between fEEG and nEEG signals,[11] their extracted features were expected to exhibit significant resemblances, and therefore, nEEG was used as a surrogate for fEEG. To represent the noise in the mcEEG signals, the mother's ECG (mECG) was used, as it is the most prominent interfering signal. The following methods were employed: In the first stage, a statistical comparison was performed on the features extracted from nEEG and mECG signals. The Mann–Whitney U test[25] was used for this analysis because it is a non-parametric test that compares differences between two independent groups. This test is particularly useful when the data does not follow a specific distribution. The p-value for each feature was calculated to determine statistical significance. In addition, Cliff's delta was employed as a measure of effect size, providing insight into the magnitude of the difference between the two groups. The functions "ranksum" and "meanEffectSize" were used in MATLAB. This approach enables the identification of individual features that effectively distinguish nEEG from mECG.

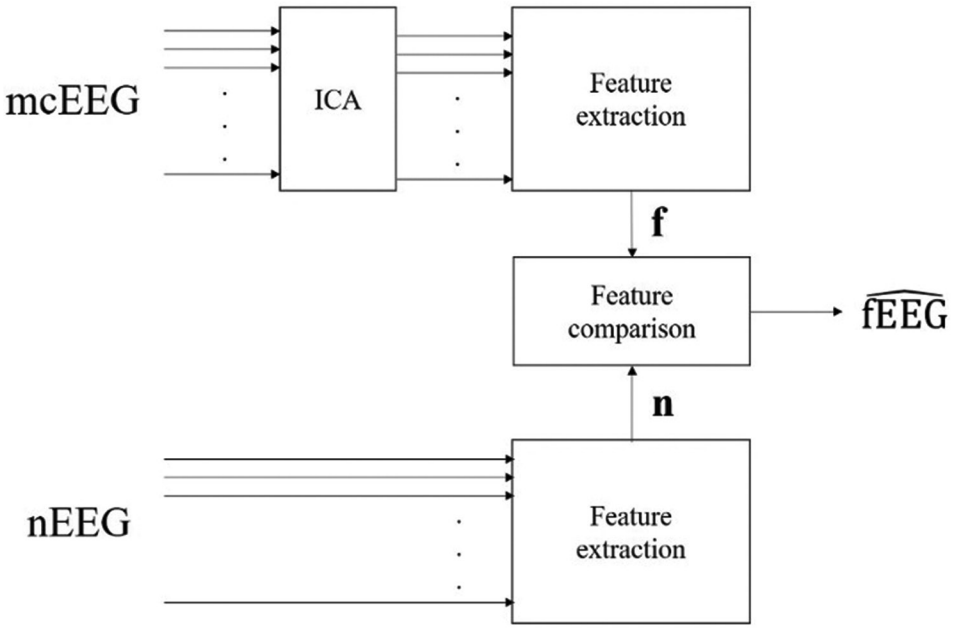

Figure 2. Block diagram of the general fEEG estimation and enhancement system
Abbreviations: fEEG: Fetal electroencephalogram; ICA: Independent component analysis; mcEEG: Multi-channel electroencephalogram; nEEG: Neonatal electroencephalogram.

However, it does not determine the optimal set of features. To address the limitation of selecting features one-by-one, a second approach was employed: Sequential forward selection (SFS) based on the k-nearest neighbors (kNN) algorithm. SFS is a bottom-up search algorithm that iteratively adds features to an empty set, selecting the feature that maximizes model performance at each step.[26] The iterative process was conducted by minimizing the misclassification error (MCE), defined as the ratio of the number of misclassified samples to the total number of samples, which was used as the performance metric (Equation 13):

$$MCE = \frac{1}{N}\sum_{i=1}^{N} I(\hat{\mathbf{y}}_i \neq \mathbf{y}_i) \quad (13)$$

where N is the total number of samples, $\hat{\mathbf{y}}_i$ and $\mathbf{y}_i$ denote the predicted class label and true class for the i-th sample, respectively, and I is an indicator function that equals 1 when $\hat{\mathbf{y}}_i$ does not equal y_i and 0 otherwise.

To ensure robust feature selection, the MCE was evaluated using leave-one-out cross-validation (LOOCV). In LOOCV, two-patient groups (one mother and one neonate) were used as the test, while the remaining patients were used to train the model. This process was repeated for each patient, and the average MCE was calculated.

The kNN algorithm was used as the model for feature evaluation, with k = 9 (the number of nearest neighbors). The kNN algorithm assigns a class to a sample based on the majority class of its kNN in the feature space, with the distance between samples measured using Euclidean distance.[27] This method allowed us to select a set of features that together optimize the discrimination between nEEG and mECG signals. This was performed using the "fitcknn" function in MATLAB.

After identifying the optimal feature set for fEEG estimation and enhancement, the features extracted from the same individual as a fetus and as a newborn were compared. It is hypothesized that there is a higher degree of similarity between the feature vectors of nEEG (n) and fEEG (f) in contrast to the features derived from other sources, such as mECG. Thus, the system as depicted in Figure 2 compares the feature vectors n and f based on the mean square error (MSE)[28] criterion (Equation 14) and adjusts the fEEG estimation from the mcEEG accordingly.

$$MSE = \frac{1}{N}\sum_{i=1}^{N}\left(\hat{\mathbf{y}}_i - \mathbf{y}_i\right)^2 \quad (14)$$

where $\hat{\mathbf{y}}_i$ is the predicted value, $\mathbf{y}_i$ represents the actual value, and N denotes the number of observations.

2.5.1. Statistical analysis

The normality of the abdominal EEG activity was assessed using normal distribution attributes, skewness, kurtosis, and inverse normal plot. Given that the pre- and post-natal EEG data were not independent, the McNemar test was

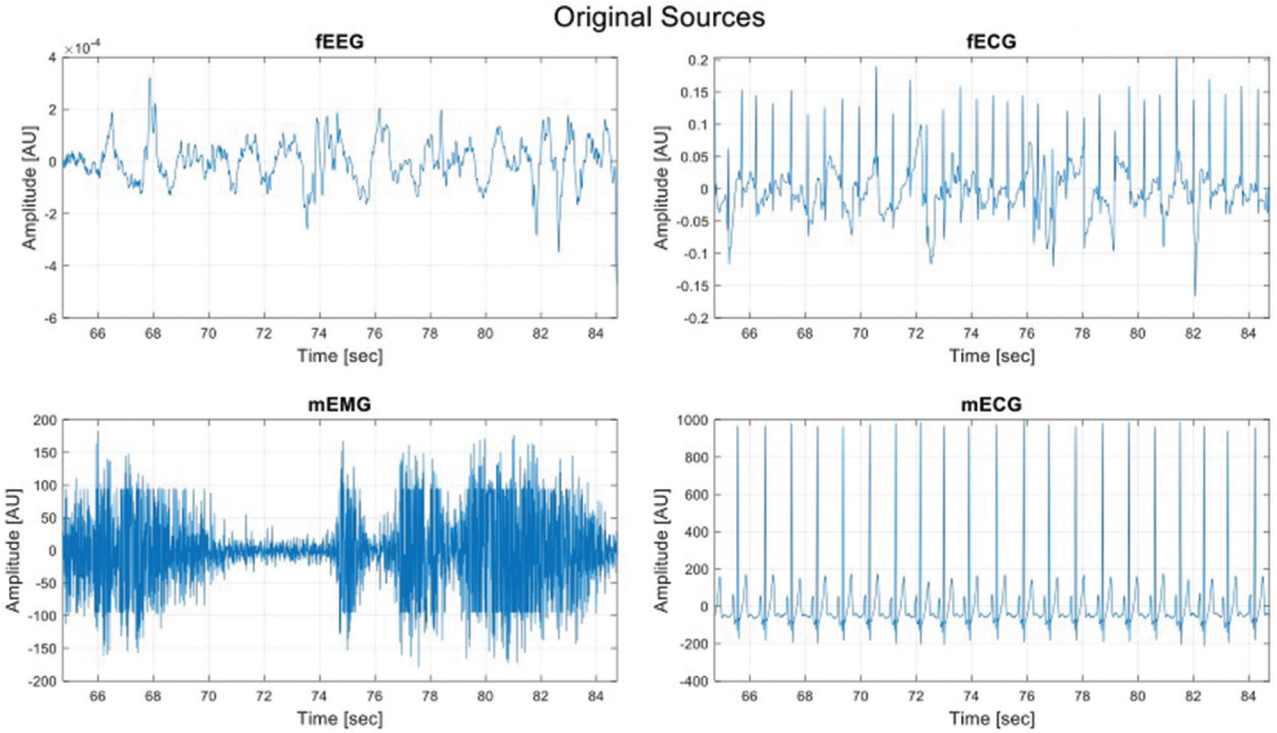

Figure 3. Original signals of fetal electroencephalogram (fEEG; top left), fetal electrocardiogram (fECG; top right), mother's electromyogram (mEMG; bottom left), and mother's electrocardiogram (mECG; bottom right) before mixing

used for dichotomous variables, and the paired *t*-test or Wilcoxon signed-rank test was employed for continuous variables. The study aimed to develop a sensitive EEG reader based on state-of-the-art electrodes and to record the fetal brain activity trans-abdominally, as reflected in its EEG patterns, by employing cutting-edge machine learning and analysis algorithms. These recordings were expected to be comparable to postnatal nEEG recordings.

2.5.2. Power calculations

During the study follow-up, women underwent abdominal EEG evaluation, and the findings were summarized as means and 95% confidence interval (CI). For each time point during pregnancy, means and 95% CIs were calculated, assuming a normal distribution. Table 1 shows the maximal width of the 95% CI around the mean, given that each time point in pregnancy is represented by 30 participating women.

3. Results

3.1. Evaluation of the FastICA algorithm using synthetically mixed mcEEG signals

To simulate mcEEG signals, we utilized four sources: nEEG and ECG acquired at Soroka Hospital, and adult ECG and EMG from publicly available PhysioNet databases.[14,15] As detailed in Section 2.3, the neonatal signals were treated as fetal signals, while the adult signals represented physiological noise from mothers. Figures 3-5 illustrate one outcome of the FastICA simulation.

Figure 3 displays the original signals after amplitude adjustment to approximate the expected ratio of 0.001:1:200:1000 for fEEG: fetal ECG: mother's EMG: mECG. The signals were presented without units due to this adjustment.

In Figure 4, each graph portrays a linear combination of the four original signals with specified weights indicated above each graph. Notably, the mECG signal dominated the mixtures, with the narrow, high-amplitude R wave appearing prominently in all of them, while the fEEG signal was less pronounced due to its low amplitude.

Following the application of FastICA, Figure 5 reveals four distinct sources that visually resemble the original signals depicted in Figure 3. The ICA algorithm does not preserve the original amplitude scale of the data;[13] hence, no units are displayed in this figure. These sources were also compared to the amplitude-modified physiological signals using NMSE values (Equation 5) provided above each source. The low NMSEs (NMSE < 10^{-4}) indicate close alignments between the ICA output and the original signals, affirming the simulation's success. Thus, it is

Table 1. Maximal width of the 95% confidence interval around the mean for each electroencephalogram parameter across pregnancy

Parameters	Range (min)	Range (max)	Mean	Standard deviation	± Maximal deviation from the mean in 95% CI for *n*=30
Low voltage irregular					
Frequency	5	8	6.5	0.50	0.18
Voltage	14	35	24.5	3.50	1.25
High-voltage slow wave activity					
Frequency	0.5	4	2.25	0.58	0.21
Voltage	50	150	100	16.67	5.96
T/A					
Frequency	3	8	5.5	0.83	0.30
Duration	4	8	6	0.67	0.24
Voltage depression					
Voltage	5	10	7.5	0.83	0.30

Abbreviations: CI: Confidence interval; T/A: Temporal/Anterior.

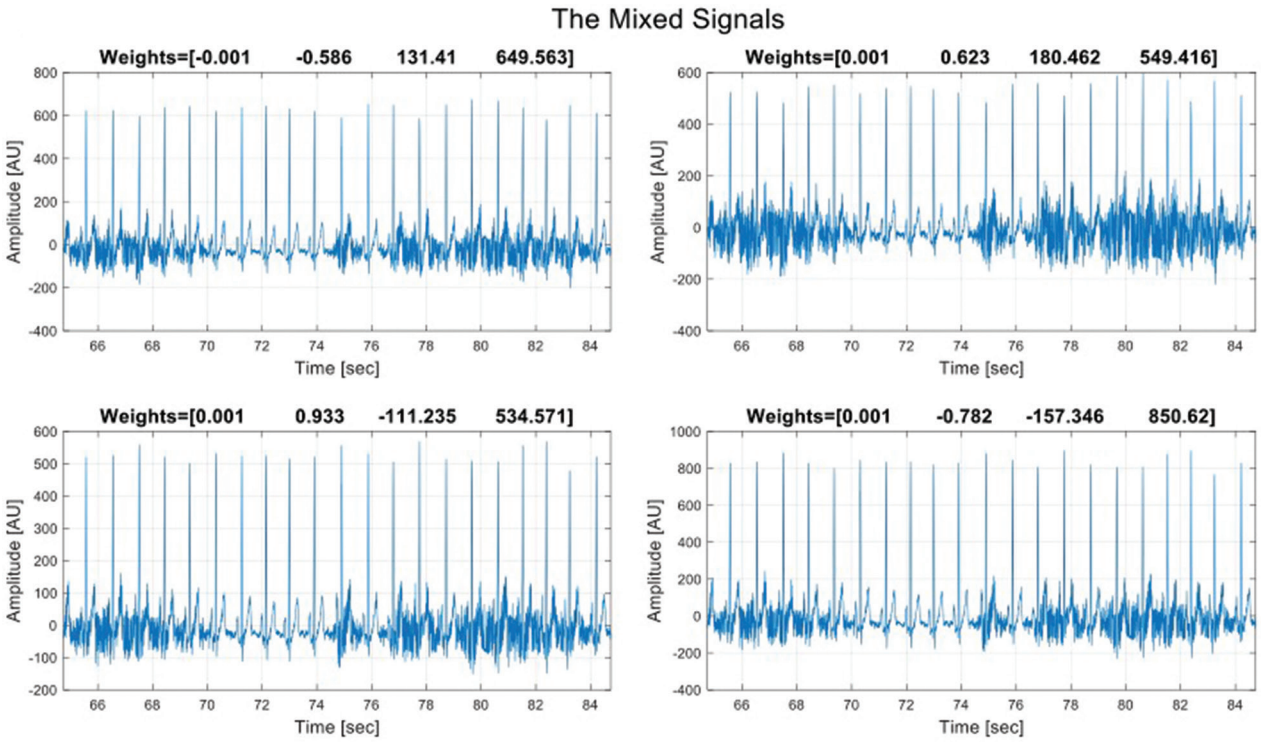

Figure 4. Mixed signals of maternal electrocardiogram (ECG) and fetal electroencephalogram (EEG) recording (above each graph mentioned the weights for each original signal, the numbers represent the weights for fetal EEG, fetal ECG, mother's electromyogram, and mother's ECG, respectively)

asserted that the FastICA algorithm can effectively process mcEEG signals and extract estimated fEEG signals.

3.2. Application of FastICA to filtered mcEEG signals for preliminary component analysis

At this stage, we applied the FastICA algorithm to the data acquired from the mother's abdomen (mcEEG). Before applying the FastICA algorithm, the data were digitally filtered as mentioned in Section 2.3 to remove noise unrelated to the EEG.

Figure 6 depicts a 20-s segment of the mcEEG signal in a bipolar presentation. The prominence of the mECG is evident, similar to the simulations, as shown in Figure 4. Next, the FastICA algorithm was applied to the data

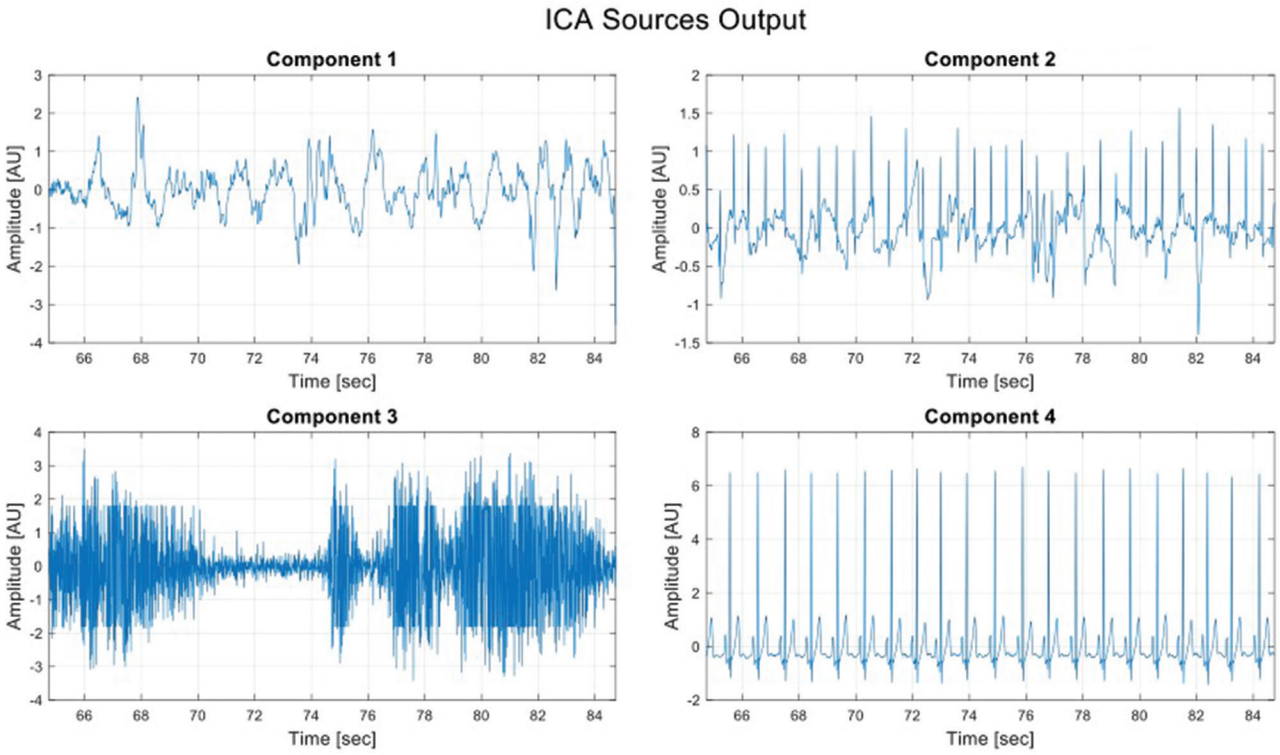

Figure 5. Independent component analysis based on the sources' output
Abbreviation: ICA: Independent component analysis.

acquired from the mother's abdomen (mcEEG).

Figure 7 presents the results after applying the ICA algorithm. Component 1 exhibited patterns resembling mECG. Components 2 and 3, on the other hand, contained patterns indicative of potential fEEG, while components 4, 5, and 6 captured various physiological or external noises.

Feature extraction and selection were performed by analyzing six mECG signals (one channel per mother) and three nEEG signals (seven channels per neonate). The features that could effectively differentiate between noise (primarily represented by mECG) and potential fEEG signals (represented by nEEG) were identified.

Figure 8 presents an example of a feature comparison, specifically the RSP across different frequency bands. Each dot in this box plot represents a 20-s segment, with the blue box plot corresponding to mECG and the red box plot to nEEG. The RSP of the δ, θ, α, and β frequency bands shows a significant difference between mECG and nEEG patterns. However, the γ frequency band exhibits a similar distribution between mECG and nEEG.

Table 2 displays the results of the Mann–Whitney *U* test of the RSP feature, including the *p*-values and Cliff's delta effect sizes for each frequency band. The δ, θ, α, and β frequency bands have low *p*-values ($<10^{-15}$) and large effect sizes (|Cliff's delta| > 0.84), indicating a highly significant difference between mECG and nEEG in terms of RSP. In contrast, the γ frequency band shows a high *p*-value (>0.05) and a much smaller effect size (|Cliff's delta| = 0.23), suggesting it is not as effective in distinguishing between the two signals.

The statistical analysis revealed that most features exhibited low *p*-values and high Cliff's delta values. However, exceptions included the γ frequency band and several AR coefficients. These findings suggest that the features listed in section 2.4 (feature extraction) are generally effective at distinguishing nEEG from mECG, indicating their potential as robust separators for fEEG and noise. The SFS was applied using the kNN algorithm with k = 9. Figure 9 illustrates the MCE as a function of the number of features selected by the SFS algorithm. The MCE reached its minimum at seven features, after which it increased, indicating overfitting. Therefore, the first seven features selected by the SFS algorithm were chosen as the optimal feature set in the following order: α bandwidth, the first two AR model coefficients (ar1, ar2), θ bandwidth, mean absolute of the first differences, SEF90, and δ bandwidth.

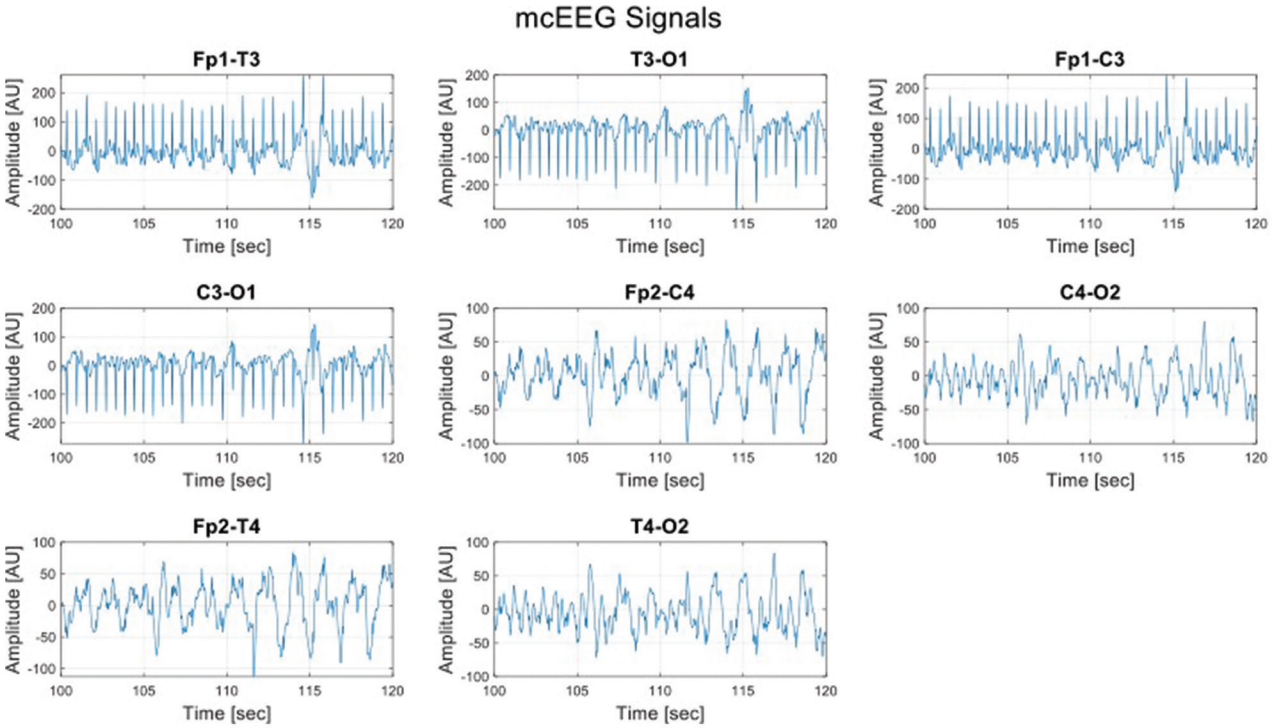

Figure 6. The mcEEG signals from different channels
Abbreviations: EEG: Electroencephalogram; mcEEG: Multi-channel electroencephalogram.

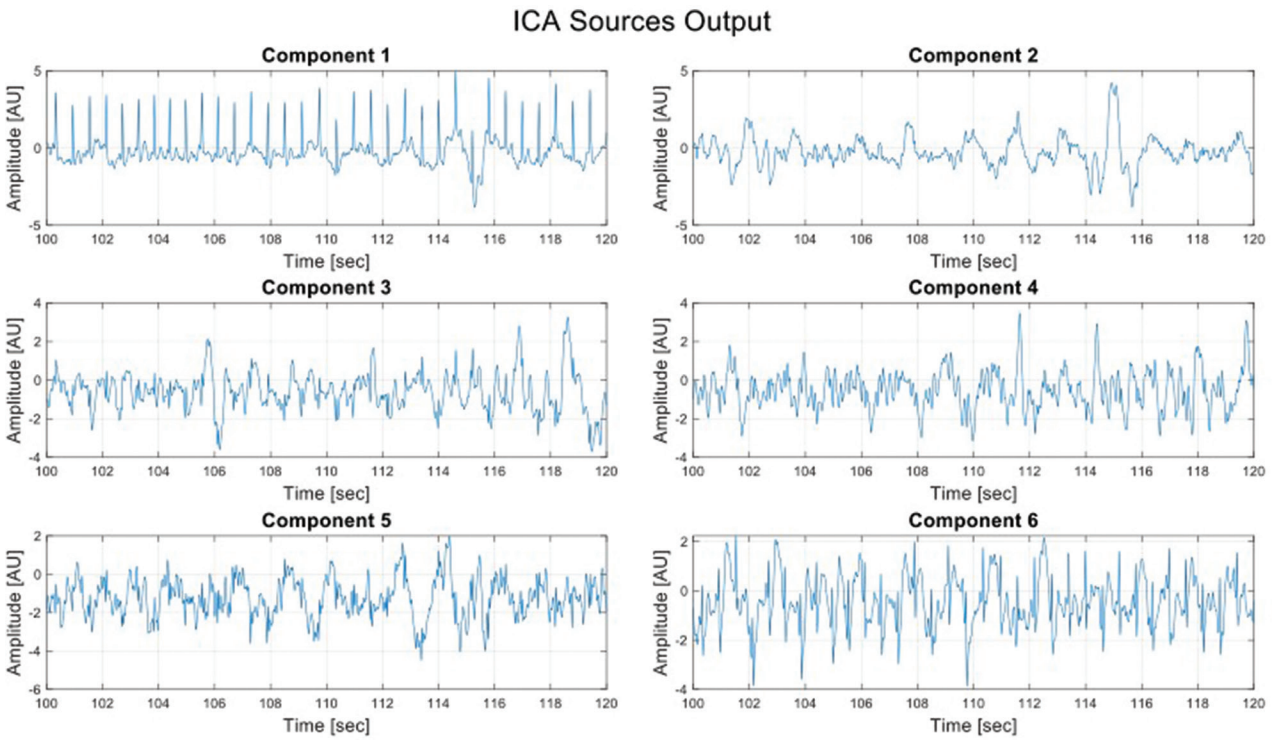

Figure 7. Independent component analysis sources output

Table 2. Mann–Whitney U test of the relative spectral power features of the difference frequency bands

Cliff's effect	*p*-value	Frequency band
0.90±0.03	$2.89\times10^{-20}\pm3.70\times10^{-19}$	δ∈[0.5,3]
−0.84±0.04	$1.12\times10^{-16}\pm1.63\times10^{-15}$	θ∈[3,8]
−0.96±0.02	$1.60\times10^{-24}\pm1.27\times10^{-23}$	α∈[8,15]
−0.97±0.02	$3.07\times10^{-25}\pm1.36\times10^{-24}$	β∈[15,30]
−0.23±0.08	0.06±0.12	γ∈[30,48]

3.3. Validation of the estimated fEEG through comparison with nEEG

These selected features based on MCE were utilized to compare ICA output sources with nEEG recordings from the same neonate to assess their similarity in characteristics.

Figure 10 compares an estimated fEEG segment with an nEEG segment in both the time (left) and frequency (right) domains. The similarity between these segments was assessed using the MSE criterion (Equation 14), with the feature comparison yielding values below the MSE threshold of 4×10^{-4}. In the frequency domain, significant similarities were evident through non-parametric estimations (shown in blue) for each signal segment, with dashed gray lines marking the brain wave bands δ, θ, α, β, and γ. Similarities were also apparent in the time domain, where the patterns of the estimated fEEG (top) and nEEG (bottom) exhibited clear resemblance. These recordings were obtained using the Bio-Logic Netlink device, which does not permit proper extraction of unit information. Therefore, the time domain signals are presented without units. To validate these findings, these results were reviewed by our nEEG experts, who confirmed the potential presence of fetal brain activity.

4. Discussion

We developed signal-processing and data-analysis methods to extract fEEG signals from maternal abdominal mcEEG recordings obtained before delivery. This work may potentially advance prenatal care by enabling early detection and intervention for neurodevelopmental disorders. Our approach combined digital filters, ICA, and feature-extraction-selection techniques to analyze the signals recorded from the maternal abdomen to potentially isolate fEEG signals.

The primary challenge of this project lies in the inherently low SNR of fEEG signals due to substantial maternal and environmental noise and the distance between the recording electrodes on the maternal abdomen and the fetal brain. The methodology effectively addressed this challenge through a sequential series of steps, including source separation using the FastICA algorithm and feature extraction from the mcEEG signal, which can serve as a potential source of fEEG and nEEG signals.

4.1. Signal preprocessing and source separation

A robust preprocessing step that included serial digital filters to remove artifacts from the raw mcEEG and nEEG signals was implemented. The FastICA algorithm proved to be an important component in these analyses, successfully separating the mixed signals into distinct sources.[29] These preliminary simulations, conducted with a combination of neonatal and adult physiological signals, demonstrated the algorithm's capability to isolate possible fEEG signals. They also showed visually distinct sources and used the NMSE criterion to quantify the accuracy of the separation, confirming high accuracy.[30]

Upon applying the FastICA algorithm to the acquired mcEEG data, the algorithm effectively separated the signals, with one of the sources displaying patterns resembling mECG. This step laid the foundation for further analysis and feature extraction, crucial for distinguishing potential fEEG signals from background noise.

However, it is important to note that ICA can be affected by amplitude scaling. While ICA is proficient at separating mixed sources based on statistical independence, it does not guarantee the preservation of the original signal amplitudes. This limitation could potentially impact the interpretation of the separated signals, particularly when amplitude information is critical for distinguishing between different signal sources. The amplitude scaling issue remains a consideration for future refinements of the method.

The source separation step is supported by both low NMSE values in simulations and the physiological plausibility of the separated components. The application of FastICA reliably distinguished recognizable cardiac activity in both simulated and real mcEEG data, increasing confidence that subtle neural signals can also be detected. In addition, the use of established artifact-removal filters ensures that source separation was achieved through true physiological differences, rather than residual noise.

4.2. Feature extraction and selection

The feature extraction process targeted both time- and frequency-domain characteristics to differentiate nEEG from mECG signals, with nEEG serving as a model for fEEG due to their known similarities and mECG serving as noise.[31]

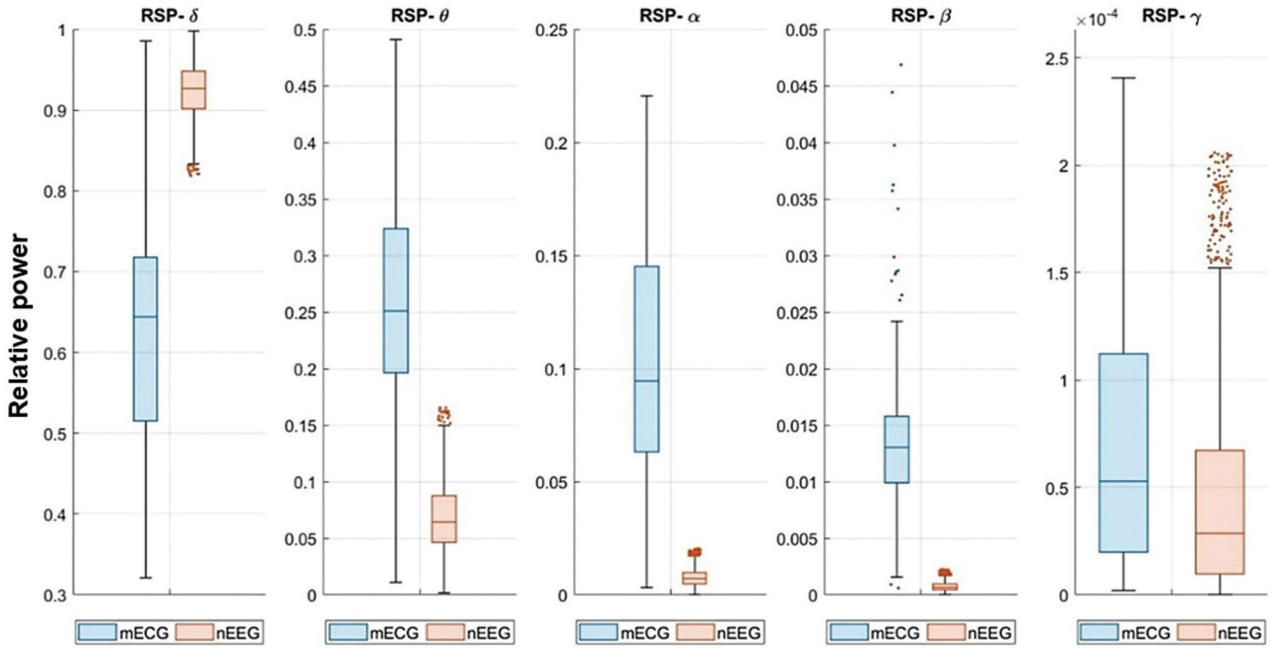

Figure 8. Relative spectral power (RSP) between neonatal electroencephalogram (nEEG) and maternal electrocardiogram (mECG) recordings

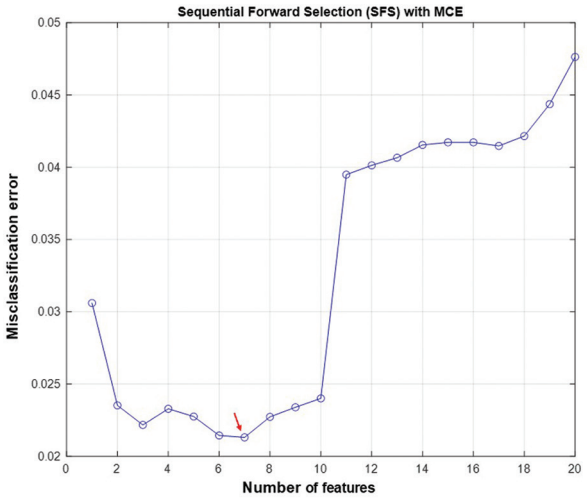

Figure 9. Sequential forward selection as a function of misclassification error (MCE) based on the number of features selected

The results show that frequency-domain features, especially in the δ, θ, α, and β bands, effectively distinguished nEEG from mECG.[3] The Mann–Whitney *U* test and Cliff's delta effect size confirmed significant differences across these bands, except for the γ band, which had a lower effect size despite a low *p*-value, indicating that it may not be an optimal feature for distinguishing noise from potential fEEG. This outcome was consistent with existing knowledge, as the physiologic γ band is primarily associated with higher cognitive functions and tends to be more prominent in brain activity during the later stages of neonatal development.[32]

SFS with kNN identified a subset of seven features – α bandwidth, AR coefficients (ar1, ar2), θ bandwidth, mean absolute of the first differences, SEF90, and δ bandwidth – as the most discriminative. These features, particularly the frequency bands and AR coefficients, are promising parameters in distinguishing potential fEEG from background noise. While SFS is not the most optimized feature selection technique (e.g., exhaustive search methods), it is time-efficient and provides strong results, avoiding the computational complexity of more exhaustive methods.

The strength of these findings is supported by their statistical significance and alignment with known nEEG physiology. The selected features correspond well with established nEEG frequency bands, enhancing their clinical credibility. The use of robust, non-parametric statistical methods minimizes the risk of false associations. In addition, validating feature selection with LOOCV reduced the risk of overfitting, supporting the generalizability and potential clinical utility of the extracted features.

4.3. Validation of estimated fEEG

Using the fetal-neonatal dyad approach, in which each neonate is the control for its recording as a fetus, we applied the optimal set of features, identified through SFS, to compare the estimated fEEG signals extracted from the

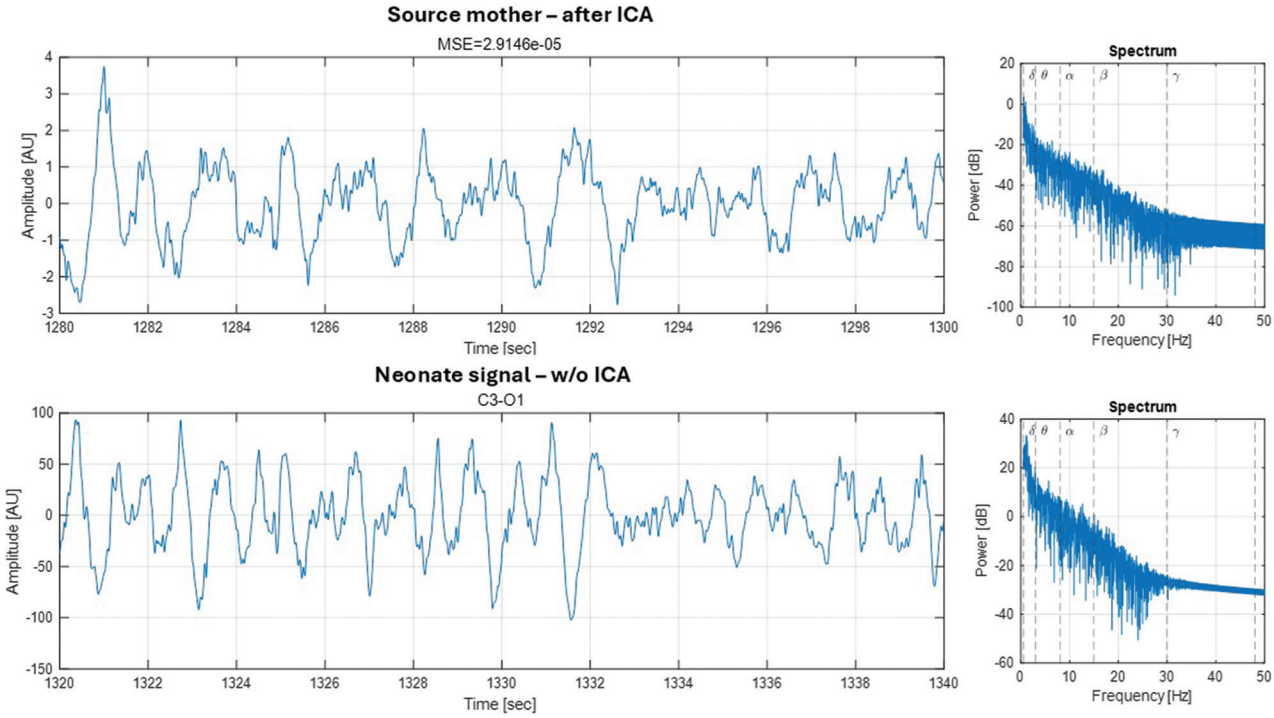

Figure 10. Comparison between abdominal (top) and neonatal (bottom) EEG using the chosen feature vector, in the time domain (left) and the frequency domain (right)
Abbreviations: EEG: Electroencephalogram; ICA: Independent component analysis; MSE: Mean square error.

maternal abdominal recordings (mcEEG) with the nEEG signals recorded post-delivery from the same neonate. The analysis revealed several 20-s segments in which the extracted features showed significant similarities in both the time and frequency domains between the estimated fEEG and nEEG. These similarities were particularly evident in segments with low MSE values, indicating a close match between the two signal types.

Further validation of these findings was supported by expert review. Specialists in nEEG analysis examined these low MSE segments and identified characteristics consistent with fEEG signals. Their assessment highlights the potential of our method to isolate genuine fEEG signals from the noisy mcEEG recordings, providing a non-invasive approach for monitoring fetal brain activity.

The strength of this validation comes from the combination of quantitative (low MSE values), within-subject comparisons (fetal-neonatal dyads), and expert clinical review. This approach minimizes the chance that observed similarities are due to random associations or maternal contamination. By using each neonate as its own control, we control for inter-individual variability and further support that the detected signals reflect true fetal brain activity.

In addition, both the spectral and amplitude trends, as well as the algorithm-identified artifact components, closely resembled those reported in similar studies. This indicates that the implemented method provides a reliable and meaningful representation of the underlying fEEG signals. The performance of ICA on recordings obtained from different approaches can serve as an indicator of the proposed algorithm's adaptability to varying environments and recording conditions. Achieving consistent results across different equipment in this study demonstrates the robustness of the method under diverse circumstances. Although the dataset was limited to a relatively small number of subjects, the consistency of the extracted fEEG features across recordings suggests that the findings are not restricted to a single observation, subject, or condition. This supports the potential generalizability of the proposed method to a broader population, although further study on larger datasets is needed to strengthen this conclusion.

4.4. Limitations

Despite the promising results, several limitations must be acknowledged. The reliance on nEEG as a reference for fEEG, while supported by previous publications and experts' opinions, introduces a degree of uncertainty, as actual fEEG signals may exhibit variations that were

previously unknown, since such recordings are not currently available.[33,34]

Moreover, while ICA demonstrated its utility for signal separation, the quality of the extracted components heavily depends on the number and placement of electrodes, as well as the characteristics of the maternal abdomen.[35] Future studies could investigate the use of advanced ICA variants or alternative blind source separation techniques to enhance the robustness of signal extraction and handle the scaling issue.

Furthermore, one of the major challenges in the noninvasive extraction of the fEEG signal is its exceptionally low amplitude. This limitation arises from signal attenuation as it passes through multiple tissue layers, including the fetal skull, amniotic fluid, uterine wall, and maternal abdomen. The distance between the fetal head and the maternal abdominal surface can reduce the signal below the detection threshold of currently available electrodes. Therefore, the development of fEEG technology will require not only advanced signal processing techniques but also the design of electrodes with higher sensitivity to compensate for this significant signal decay.

In addition, this study did not account for potentially influential factors, such as gestational age, behavioral states, or sleep–wake cycles at the time of data collection. These variables are known to affect nEEG and could therefore introduce bias. Future studies with larger cohorts are needed to systematically evaluate the influence of those variables on the quality and interpretability of extracted fEEG signals. Another limitation of this study is that we cannot confirm whether the same montage is used for the neonate and for the fetus. This is because the acquisition from the maternal abdomen is relative in space to the floating fetal head, while the acquisition of EEG from the neonatal head is performed via direct contact. Nevertheless, to maintain the similarity, we placed the EEG electrodes on the maternal abdomen in a configuration similar to the neonatal montage.

5. Conclusion

This study presents a non-invasive method for extracting fEEG from transabdominal multi-channel recordings from the gravid maternal abdomen using digital filtering and FastICA. Preprocessing included band-pass filtering and artifact rejection to enhance signal quality. FastICA was then applied to separate independent components, aiming to isolate fEEG with minimal maternal and environmental interference.

Validation was performed using nEEG as a reference due to the absence of fEEG recordings. Time- and frequency-domain features were extracted and refined through SFS with kNN to distinguish fetal signals from noise.

Results show that the method can identify components with fEEG-like characteristics, especially in segments with lower MSE compared to nEEG. While promising, the approach is limited by its reliance on nEEG and ICA's sensitivity to electrode setup and maternal anatomy. In conclusion, this work demonstrated a feasible approach for non-invasive fEEG extraction, with potential applications in prenatal monitoring.

Acknowledgments

We would like to thank Zipi Vasker, Noa Trifus, Shir Neubaubr, and Lee Steinberg for their contributions to EEG data collection.

Funding

This research was supported by the Ministry of Innovation, Science and Technology, Israel (grant number: 0004750).

Conflict of interest

The authors declare no competing interests.

Author contributions

Conceptualization: Offer Erez, Allon Guez
Data curation: Offer Erez, Taeer Avnon
Formal analysis: Eilon Shany, Robert Clancy
Funding acquisition: Offer Erez, Allon Guez
Investigation: Offer Erez, Yaniv Zigel, Allon Guez, Ali Nasirlou, Eden Koresh, Ophir Oren
Methodology: Yaniv Zigel, Ali Nasirlou, Eden Koresh, Ophir Oren
Supervision: Yaniv Zigel, Allon Guez, Robert Clancy, Eilon Shany
Validation: Eden Koresh, Ophir Oren
Visualization: Eden Koresh, Ophir Oren
Writing–original draft: Ali Nasirlou, Eden Koresh, Ophir Oren
Writing–review & editing: Offer Erez, Allon Guez, Ali Nasirlou, Eden Koresh, Ophir Oren, Taeer Avnon

Ethics approval and consent to participate

The study was approved by the local institutional review board at Soroka University Medical Center (approval ID: IRB-0009-23-SOR). Written informed consent was obtained from all individual participants included in the study. Additionally, written informed consent for neonates was obtained from the parents.

Consent for publication

The study was approved by the Institutional Review Board, which authorized the publication of deidentified patient data; therefore, explicit participant consent was not required.

Availability of data

Data are available upon request through the corresponding author.

References

1. Buss C, Entringer S, Swanson JM, Wadhwa PD. The role of stress in brain development: The gestational environment's long-term effects on the brain. *Cerebrum*. 2012;2012:4.
2. Wu Y, Lu YC, Jacobs M, *et al*. Association of prenatal maternal psychological distress with fetal brain growth, metabolism, and cortical maturation. *JAMA Netw Open*. 2020;3(1):e1919940.

   doi: 10.1001/jamanetworkopen.2019.19940
3. Castel A, Frank YS, Feltner J, Karp FB, Albright CM, Frasch MG. Monitoring fetal electroencephalogram intrapartum: A systematic literature review. *Front Pediatr*. 2020;8:584.

   doi: 10.3389/fped.2020.00584
4. Fitzgerald E, Hor K, Drake AJ. Maternal influences on fetal brain development: The role of nutrition, infection and stress, and the potential for intergenerational consequences. *Early Hum Dev*. 2020;150:105190.

   doi: 10.1016/j.earlhumdev.2020.105190
5. Paz-Levy D, Schreiber L, Erez O, *et al*. Inflammatory and vascular placental lesions are associated with neonatal amplitude integrated EEG recording in early premature neonates. *PLOS One*. 2017;12(6):e0179481.

   doi: 10.1371/journal.pone.0179481
6. Van Den Heuvel MI. From the Womb into the World: Protecting the fetal brain from maternal stress during pregnancy. *Policy Insights Behav Brain Sci*. 2022;9(1):96-103.

   doi: 10.1177/23727322211068024
7. Lindsley DB. Heart and brain potentials of human fetuses in utero. By Donald B. Lindsley, 1942. *Am J Psychol*. 1942;55(3):412-416.

   doi: 10.2307/1417473
8. Bernstine RL, Borkowski WJ, Price AH. Prenatal fetal electroencephalography. *Am J Obstet Gynecol*. 1955;70(3):623-630.

   doi: 10.1016/0002-9378(55)90357-4
9. Rosen MG, Scibetta JJ, Hochberg CJ. Human fetal electroencephalogram. 3. Pattern changes in presence of fetal heart rate alterations and after use of maternal medications. *Obstet Gynecol*. 1970;36(1):132-140.
10. Eswaran H, Wilson JD, Lowery CL, *et al*. Brain stem auditory evoked potentials in the human fetus during labor. *Am J Obstet Gynecol*. 1999;180(6):1422-1426.

    doi: 10.1016/S0002-9378(99)70029-3
11. Abbasi H, Battin MR, Butler R, *et al*. Early signatures of brain injury in the preterm neonatal EEG. *Signals*. 2023;4(3):630-643.

    doi: 10.3390/signals4030034
12. Nayak CS, Anilkumar AC. Neonatal EEG. In: *StatPearls*. Tresure Islandm, FL: StatPearls Publishing; 2024.
13. Hyvärinen A, Oja E. Independent component analysis: Algorithms and applications. *Neural Networks*. 2000;13(4-5):411-430.

    doi: 10.1016/S0893-6080(00)00026-5
14. García-González MA, Argelagós-Palau A, Fernández-Chimeno M, Ramos-Castro J. *A Comparison of Heartbeat Detectors for the Seismocardiogram, Computing in Cardiology 2013*. Zaragoza, Spain: IEEE; 2013. p. 461-464.
15. Study TSHH. *Sleep Heart Health Study Polysomnography Database*. Oxford: Oxford Acadmic; 2003.

    doi: 10.13026/C2MK5F
16. Peterfi I, Kellenyi L, Szilagyi A. Noninvasive recording of true-to-form fetal ECG during the third trimester of pregnancy. *Obstet Gynecol Int*. 2014;2014:285636.

    doi: 10.1155/2014/285636
17. Butler HL, Newell R, Hubley-Kozey CL, Kozey JW. The interpretation of abdominal wall muscle recruitment strategies change when the electrocardiogram (ECG) is removed from the electromyogram (EMG). *J Electromyogr Kinesiol*. 2009;19(2):e102-e113.

    doi: 10.1016/j.jelekin.2007.10.004
18. Abdulla W, Wong L. Neonatal EEG signal characteristics using time frequency analysis. *Phys A Statis Mech Applic*. 2011;390(6):1096-1110.

    doi: 10.1016/j.physa.2010.11.013
19. Rosen MG, Scibetta JJ. The human fetal electroencephalogram. I. An electrode for continuous recording during labor. *Am J Obstet Gynecol*. 1969;104(7):1057-1060.

    doi: 10.1016/0002-9378(69)90703-0
20. Borgstedt AD, Rosen MG, Chik L, Sokol RJ, Bachelder L, Leo P. Fetal electroencephalography. Relationship to neonatal and one-year developmental neurological examinations in high-risk infants. *Am J Dis Child*. 1975;129(1):35-38.

    doi: 10.1001/archpedi.1975.02120380021006
21. Lundy C, Boylan GB, Mathieson S, Proietti J, O'Toole JM. Quantitative analysis of high-frequency activity in neonatal EEG. *Comput Biol Med*. 2023;165:107468.

    doi: 10.1016/j.compbiomed.2023.107468
22. Atyabi A, Shic F, Naples A. Mixture of autoregressive modeling orders and its implication on single trial EEG classification. *Expert Syst Appl*. 2016;65:164-180.

doi: 10.1016/j.eswa.2016.08.044

23. Boonyakitanont P, Lek-uthai A, Chomtho K, Songsiri J. A review of feature extraction and performance evaluation in epileptic seizure detection using EEG. *Biomed Signal Process Control*. 2020;57:101702.

    doi: 10.1016/j.bspc.2019.101702

24. Thaler I, Boldes R, Timor-Tritsch I. Real-time spectral analysis of the fetal EEG: A new approach to monitoring sleep states and fetal condition during labor. *Pediatr Res*. 2000;48(3):340-345.

    doi: 10.1203/00006450-200009000-00013

25. McKnight PE, Najab J. Mann-whitney U test. In: *The Corsini Encyclopedia of Psychology*. United States: Wiley; 2010. p. 1-1.

    doi: 10.1002/9780470479216.corpsy0524

26. Marcano-Cedeño A, Quintanilla-Domínguez J, Cortina-Januchs MG, Andina D. Feature Selection using Sequential Forward Selection and Classification Applying Artificial Metaplasticity Neural Network. In: *IECON 2010 - 36th Annual Conference on IEEE Industrial Electronics Society*. United States: IEEE; 2010. p. 2845-2850.

    doi: 10.1109/IECON.2010.5675075

27. Kramer O. K-nearest neighbors. In: Kramer O, editor. *Dimensionality Reduction with Unsupervised Nearest Neighbors*. Berlin: Springer; 2013. p. 13-23.

    doi: 10.1007/978-3-642-38652-7_2

28. Poli AA, Cirillo MC. On the use of the normalized mean square error in evaluating dispersion model performance. *Atmos Environ Part A Gen Topics*. 1993;27(15):2427-2434.

    doi: 10.1016/0960-1686(93)90410-Z

29. Yuan L, Zhou Z, Yuan Y, Wu S. An improved fastICA method for fetal ECG extraction. *Comput Math Methods Med*. 2018;2018:7061456.

    doi: 10.1155/2018/7061456

30. Taheri N, Kachenoura A, Ansari-Asl K, *et al*. Feasibility of blind source separation methods for the denoising of dense-array EEG. In: *2015 37th Annual International Conference of the IEEE Engineering in Medicine and Biology Society (EMBC)*. United States: IEEE; 2015. p. 4773-4776.

    doi: 10.1109/EMBC.2015.7319461

31. Haddad N, Govindan RB, Vairavan S, *et al*. Correlation between fetal brain activity patterns and behavioral states: An exploratory fetal magnetoencephalography study. *Exp Neurol*. 2011;228(2):200-205.

    doi: 10.1016/j.expneurol.2011.01.003

32. Tierney A, Strait DL, O'Connell S, Kraus N. Developmental changes in resting gamma power from age three to adulthood. *Clin Neurophysiol*. 2013;124(5): 1040-1042.

    doi: 10.1016/j.clinph.2012.09.023

33. Sokol RJ, Rosen MG. The fetal electroencephalogram. *Clin Obstet Gynaecol*. 1974;1(1):123-138.

    doi: 10.1016/S0306-3356(21)00499-4

34. Castro Conde JR, González Campo C, González González NL, *et al*. Assessment of neonatal EEG background and neurodevelopment in full-term small for their gestational age infants. *Pediatr Res*. 2020;88(1):91-99.

    doi: 10.1038/s41390-019-0693-0

35. Rooijakkers MJ, Song S, Rabotti C, *et al*. Influence of electrode placement on signal quality for ambulatory pregnancy monitoring. *Comput Math Methods Med*. 2014;2014:960980.

    doi: 10.1155/2014/960980